Cch1 Restores Intracellular Ca²⁺ in Fungal Cells during Endoplasmic Reticulum Stress*

Min-Pyo Hong, Kiem Vu, Jennifer Bautos, and Angie Gelli[1]

From the Department of Pharmacology, School of Medicine, University of California, Davis, California 95616

Pathogens endure and proliferate during infection by exquisitely coping with the many stresses imposed by the host to prevent pathogen survival. Recent evidence has shown that fungal pathogens and yeast respond to insults to the endoplasmic reticulum (ER) by initiating Ca^{2+} influx across their plasma membrane. Although the high affinity Ca^{2+} channel, Cch1, and its subunit Mid1, have been suggested as the protein complex responsible for mediating Ca^{2+} influx, a direct demonstration of the gating mechanism of the Cch1 channel remains elusive. In this first mechanistic study of Cch1 channel activity we show that the Cch1 channel from the model human fungal pathogen, *Cryptococcus neoformans*, is directly activated by the depletion of intracellular Ca^{2+} stores. Electrophysiological analysis revealed that agents that enable ER Ca^{2+} store depletion promote the development of whole cell inward Ca^{2+} currents through Cch1 that are effectively blocked by La^{3+} and dependent on the presence of Mid1. Cch1 is permeable to both Ca^{2+} and Ba^{2+}; however, unexpectedly, in contrast to Ca^{2+} currents, Ba^{2+} currents are steeply voltage-dependent. Cch1 maintains a strong Ca^{2+} selectivity even in the presence of high concentrations of monovalent ions. Single channel analysis indicated that Cch1 channel conductance is small, similar to that reported for the Ca^{2+} current I_{CRAC}. This study demonstrates that Cch1 functions as a store-operated Ca^{2+}-selective channel that is gated by intracellular Ca^{2+} depletion. The inability of cryptococcal cells that lacked the Cch1-Mid1 channel to survive ER stress suggests that Cch1 and its co-regulator, Mid1, are critical players in the restoration of Ca^{2+} homeostasis.

Store-operated Ca^{2+} (SOC)[2] entry is a process whereby Ca^{2+} influx across the eukaryotic plasma membrane results from the depletion of Ca^{2+} from endoplasmic reticulum (ER) stores (1–6). Stresses imposed on the ER can promote a prolonged depletion of Ca^{2+} that will lead to cell death unless ER Ca^{2+} levels are replenished (1–3). All lower eukaryotes including the model fungal pathogen, *Cryptococcus neoformans*, express the Cch1-Mid1 channel (CMC) in their plasma membrane (7–11). *C. neoformans* is a primary human pathogen because it causes

life-threatening meningitis primarily in immunocompromised patients (12, 13). Its ability to survive in low $[Ca^{2+}]$ environments is dependent on the combined activity of Cch1, the predicted pore of the channel complex, and Mid1, a binding partner of Cch1 (7, 14, 20). Genetic analysis has indicated that strains of *C. neoformans* lacking *CCH1* or *MID1* were not viable in conditions of limiting extracellular $[Ca^{2+}]$, consistent with its role as the only high affinity Ca^{2+} channel in the plasma membrane (7, 14).

Treatment of fungal cells with azole antifungals led to an influx of extracellular Ca^{2+} that promoted the survival of fungi exposed to azole-induced stress (16–19). Because azoles promote ER stress by blocking ergosterol biosynthesis, it had been proposed that the depleted state of Ca^{2+} stores might activate CMC where it could then function to refill Ca^{2+} stores (16, 17). This notion was reinforced by experiments demonstrating that changes in secretory Ca^{2+} levels promoted the influx of extracellular $^{45}Ca^{2+}$ possibly through CMC in yeast (20); however, the gating mechanism of Cch1 channel activity has yet to be established.

Resolving channel gating is best accomplished by patch clamp techniques because these techniques can successfully determine specific kinetic parameters of ion channels such as channel selectivity, channel conductance, and activation kinetics (21). We had previously applied patch clamp techniques directly to isolated spheroplasts of *C. neoformans* to resolve Cch1 function by measuring Cch1 channel activity straightaway; however, this approach was burdened with many technical difficulties that led to inconsistencies in Cch1 channel measurements. Consequently, the expression of Cch1 in a heterologous expression system such as the HEK293 (human embryonic kidney) mammalian cell line appeared to be the best approach that would permit direct functional analysis of the Cch1 channel. Unfortunately, the measurement of Cch1 channel activity in a heterologous expression system had been impossible until recently because of the significant challenge posed by the molecular cloning of *CCH1* as a result of the toxicity of the *CCH1* gene or gene product in *Escherichia coli* cells (8). For this reason, standard molecular biological techniques that used *E. coli* as a host could not be used, and therefore we devised a new approach that ultimately led to the successful cloning of *CCH1* and its functional expression (22).

In the present study we report the first electrophysiological characterization and mechanistic study of Cch1 channel activity. The functional expression of Cch1 along with its subunit Mid1 revealed that the Cch1 channel is directly activated by ER-stressing agents that deplete ER Ca^{2+} levels, suggesting that Cch1 is gated by the passive depletion of intracellular Ca^{2+} and

---

[1] To whom correspondence should be addressed: 451 Health Science Dr., Genome and Biomedical Science Facility, Davis, CA 95616. Fax: 530-752-7393; E-mail: acgelli@ucdavis.edu.

[2] The abbreviations used are: SOC, store-operated Ca^{2+}; ER, endoplasmic reticulum; CMC, Cch1-Mid1 channel; BAPTA, 1,2-bis(2-aminophenoxy)-ethane-*N,N,N′,N′*-tetraacetic acid cesium salt; BAPTA-AM, BAPTA tetraacetoxymethyl ester; GFP, green fluorescent protein; CRAC, Ca^{2+} release activated Ca^{2+}.

that it functions primarily to restore Ca^{2+} homeostasis. Consequently, cryptococcal cells that lacked the Cch1 channel could not survive ER stress, suggesting a critical physiological requirement for CMC.

EXPERIMENTAL PROCEDURES

Cell Culture and Reagents—All *C. neoformans* var. *grubii* strains (H99 *MATa* serotype A) were recovered from 15% glycerol stocks stored at −80 °C prior to use in these experiments. The *cch1Δ* null mutant strain was constructed previously (7). Strains were maintained on YPD (1% yeast extract, 2% peptone, and 2% dextrose) medium. Cells of *C. neoformans* were cultured in YPD medium at 30 °C for 24 h. Cells from the HEK293 cell line were cultured in Dulbecco's modified Eagle's medium with 10% calf serum and antibiotics in a 5% CO_2 incubator at 37 °C. HEK293 cells were purchased from ATCC (CRL-1573). Where indicated, a cell-impermeable form of BAPTA (Invitrogen) was added to YPD. Tunicamycin, fluconazole, and ketoconazole (Sigma-Aldrich) were dissolved in dimethyl sulfoxide at the concentrations noted in the figure legends. Thapsigargin and BAPTA-AM were purchased from Calbiochem and BAPTA from Invitrogen.

Construction of the Null Mutant Strains—Gene disruption cassettes were generated to knock down Mid1 and create the *mid1Δ* single mutant and the *cch1Δmid1Δ* double mutant. The *URA5* (uracil) nutritional marker was amplified by PCR (with primers: Ura5-Ssp1-F: CCC AATATT gatcttgggg atggtattga and Ura5R-Ssp1-R: CCC AATATT gatcccagtactacccgctc) and cloned into the middle of pCR2.1-*MID1* vector to disrupt the *MID1* open reading frame. This disruption cassette was transferred to a wild type *C. neoformans* strain by biolistic transformation as described previously (23). Colonies appeared after 3 days on −*URA* dropout medium (0.01% adenine, 0.2% yeast synthetic dropout medium without uracil, 0.5% ammonium sulfate, 0.17% yeast nitrogen base without amino acids and ammonium sulfate, 2% Bacto Agar) supplemented with 1 M sorbitol. The *mid1Δ* mutant strain was confirmed by PCR. Southern blot analysis was performed to confirm a single integration in the knock-out strain.

A similar approach was taken to construct the *cch1Δmid1Δ* double mutant strain; however, in this case the *NAT* marker was used to disrupt the *MID1* coding region. The disruption cassette was transformed into a *cch1Δ* single mutant strain by biolistic transformation. Colonies appeared after 3 days on YPD + 1 M sorbitol agar plates supplemented with 0.1 mg/ml *NAT* plates. The *cch1Δmid1Δ* mutant strain was confirmed by PCR and Southern blot analysis.

Plasmids and Transfection—We had determined previously that the *CCH1* gene from *C. neoformans* could not be cloned by standard ligation-mediated techniques that used *E. coli* as a host because the gene encoding Cch1 or possibly the gene product is toxic to *E. coli*. We have devised an alternative approach to clone *CCH1* cDNA into the pcDNA3.1/CT-GFP-topo expression plasmid under the control of the constitutive mammalian cytomegalovirus promoter (Invitrogen) that bypassed the conventional enzyme-mediated ligation reactions in *E. coli*. The approach we used to clone *CCH1* successfully has been described elsewhere (22). The Cch1 channel protein was tagged

with a C-terminal GFP instead of an N-terminal GFP to avoid interfering with the localization of Cch1 to the plasma membrane of HEK293 cells. A nontagged version of a Cch1 plasmid was also constructed and used as a control to assess the effect of the GFP fusion on the kinetics of Cch1. *MID1* was cloned into the pcDNA3.1/CT-GFP-topo expression plasmid using conventional molecular biological techniques. The *MID1* amplicon was generated from cDNA that was synthesized by the SuperScript III First-Strand synthesis system for RT-PCR (Invitrogen) using total RNA as template with the following primers: Mid-1F: atgccagcga gagaggtgta, Mid-1R: ctatccgtta-caccatctat. RNA was isolated from a culture (∼5×10^7 cells) of a wild type strain of *C. neoformans* var. *grubii* (H99). Cells were lysed with acid-washed glass beads, and total RNA was isolated and purified according to the manufacturer's instructions (RNeasy kit; Qiagen). Following blue/white colony selection, positive transformants were isolated and sequenced.

HEK293 cells were counted and trypsinized 24 h before transfection. Approximated 1.25×10^5 in 1 ml of complete medium were plated/well such that the cell density was ∼50–80% confluent on the day of transfection. Transient transfection of HEK293 cells with *CCH1-GFP* plasmid DNA and *MID1* was performed with Lipofectamine 2000 and Plus reagents according to the manufacturer's instructions (Invitrogen). Approximately 1 µg of *CCH1-GFP* and *MID1* plasmid DNA was added to 100 µl of Opti-MEM I-reduced serum medium and mixed with 1.75 ml of Lipofectamine 2000, and the mixture was incubated for 30 min at room temperature. The mixture was added directly to HEK293 cells that had been grown in a culture dish and maintained in Dulbecco's modified Eagle's medium supplemented with 4 mM L-glutamine, 10% fetal bovine serum. HEK293 cells were maintained at 37 °C with 5% CO_2 18–24 h after transfection before assaying cells for transgene expression.

Protein Analysis—Plasma membranes from HEK293 cells expressing Cch1-GFP or Mid1-GFP were isolated according to the protocol outlined in the Qproteome plasma membrane protein kit (Qiagen). Plasma membrane preparations were separated on a 6.5% SDS-polyacrylamide gel. Western blotting for Mid1 and Cch1 was performed using a rabbit polyclonal antibody to GFP (Abcam) (1:5000) as the primary antibody followed by detection with a goat polyclonal antibody to rabbit immunoglobulin G (IgG) (1:5000) (H&L (horseradish peroxidase); Abcam).

Biotinylation of Mid1 and Cch1 was performed according to the protocol described in the Pierce cell surface biotin protein isolation kit (ThermoScientific). HEK293 cells that had been transfected with Mid1-GFP and Cch1-GFP were biotinylated according to the specifications outlined in the kit. Protein samples were separated on a 6.5% polyacrylamide gel. Western blotting for biotinylated Mid1 and Cch1 was performed as explained above.

Confocal Microscopy—To examine the localization of Mid1 and Cch1 in HEK293 cells, cells expressing plasmids containing Mid1-GFP or Cch1 were fixed in 4% paraformaldehyde for 20 min at room temperature, washed in phosphate-buffered saline and subsequently visualized with a confocal microscope. Immunofluorescence of Cch1 was performed in HEK293 cells

that had been fixed in 4% paraformaldehyde and permeabilized. A primary peptide antibody against the C terminus of Cch1 (Antibodies Inc., Davis CA) was added to HEK293 cells at a dilution of 1:500. Cch1 was visualized with a secondary antibody (1:1000) conjugated with Texas Red (Abcam). Fluorescence was examined using a Carl Zeiss LSM-5 inverted confocal microscope. Mid1 and Cch1 were examined with a 488-nm and a 568-nm laser line at $40 \times$ objective. The images were scanned and captured at a resolution of 1024×1024 pixels.

Patch Clamp Measurements—Experiments were performed using conventional whole cell and single channel patch clamp techniques (21). To measure currents through Cch1, HEK293 cells expressing Cch1 and Mid1 were visually selected based on bright GFP fluorescence. Currents were stimulated by passive Ca^{2+} store depletion with a pipette solution containing 10 μM BAPTA-AM or by activation with thapsigargin (100 μM). Recording electrodes were pulled with a vertical puller (Adams and List, New York) from borosilicate glass capillaries, coated with Sylgard, fire-polished and filled with a solution containing either BAPTA-AM or thapsigargin, 130 mM Cs^+ methane sulfonate, 5 mM $MgCl_2$, 500 μM Mg-ATP, 20 mM HEPES (pH 7.2) with CsOH. Recording electrodes had a tip resistance of ~5 $M\Omega$ when placed in the following external solution: 2, 5, or 10 mM $CaCl_2$ or $BaCl_2$, 140 mM N-methyl-D-glucamine (140 mM Na^+ methane sulfonate in divalent-free solution and free of N-methyl-D-glucamine), 10 mM glucose, 10 mM HEPES (pH 7.4) with NaOH. Whole cell currents were measured by voltage ramps (-120 to $+60$ mV lasting 200 ms) from a holding potential of -60 mV. All voltages have been corrected for liquid junction potentials. Currents were filtered at 2 kHz with a four-pole Bessel filter (Dagan) contained in the Dagan amplifier and sampled at 5 kHz. Amplifier was interfaced with a Digidata 1322A (Axon Instruments, Foster City, CA) to digitize data. All data were corrected for leak currents. For single channel measurements, the outside-out patch configuration was used. Both the extracellular and pipette solutions used for single channel recordings were the same as those used in whole cell experiments. Single channel records were obtained at voltages of -60 mV and -80 mV and sampled at 25 kHz. Currents were analyzed with pCLAMP 9.0 software (Axon) and graphed with Sigmaplot 8.0 software on an IBM 3GHz computer.

Sensitivity Spot Assays—For spot assays, four strains (wild type, $mid1\Delta$, $cch1\Delta$, and $cch1\Delta mid1\Delta$) were cultured in YPD medium overnight at 30 °C. Cultures were pelleted and resuspended in sterile H_2O. Serially diluted cells (10^6, 10^5, 10^4, 10^3, 10^2) were added to YPD agar plates supplemented with ER-stressing agents (tunicamycin, fluconazole, and ketoconazole) and to YPD plates supplemented with BAPTA plus the ER-stressing agents.

RESULTS

Cch1 and Mid1 Are Expressed in the Plasma Membrane of HEK293 Cells—To resolve Ca^{2+} currents through CMC by patch clamp techniques, HEK293 cells were co-transfected with *CCH1* and *MID1* (21). Prior to initiating the patch clamp studies, the expression and localization of CMC was examined in HEK293 cells. This heterologous expression system was chosen because previous attempts to resolve CMC-mediated Ca^{2+}
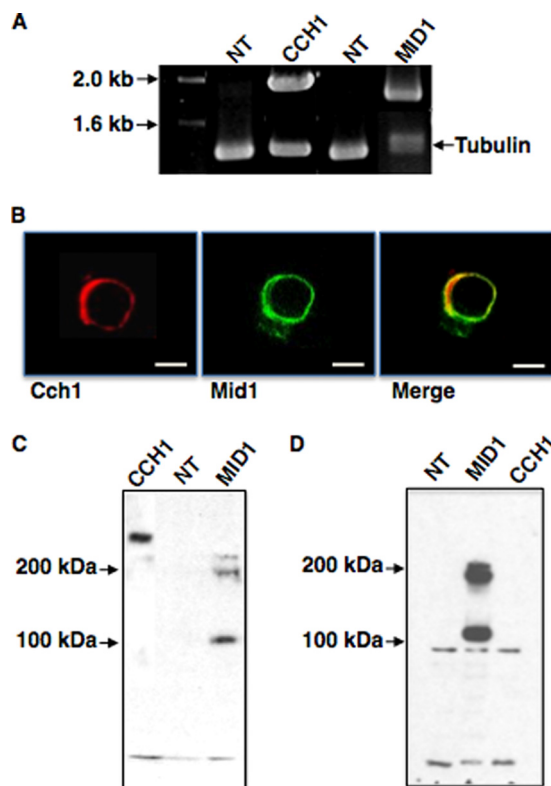
FIGURE 1. **Cch1 and Mid1 proteins are expressed in the plasma membrane of HEK293 cells.** *A*, reverse transcription-PCR analysis detected transcripts of *CCH1* and *MID1* in HEK293 cells previously transfected with CCH1 and MID1 cDNA. Transcripts were not detected in nontransfected (*NT*) cells. Tubulin is shown as a loading control. *B*, Mid1 was tagged with a C-terminal GFP tag and visualized by confocal microscopy (*center panel*). Mid1 is expressed predominantly on the cell surface of HEK293 cells, and Mid1 co-localizes with Cch1 (*right panel*, *merge*). Immunofluorescence (Texas Red) of Cch1 (nontagged) revealed a surface distribution in HEK cells (*left panel*) similar to Mid1. A primary peptide antibody to the C terminus of Cch1 and a Texas Red-conjugated secondary antibody were used to visualize Cch1. *Scale bars*, 10 μM. *C*, Western blot analysis of isolated plasma membranes from HEK293 cells expressing Cch1 or Mid1 and revealed polypeptides corresponding to the predicted sizes for Cch1 (~220 kDa) and Mid1 (monomer, ~100 kDa; complex, ~200 kDa). *D*, Western blot analysis of surface biotinylation of HEK293 cells expressing Cch1 or Mid1 revealed two distinct bands unique to the *lane* corresponding to Mid1 (monomer, ~100 kDa; complex, ~200 kDa). These bands were not detected in nontransfected HEK cells (*NT*). A protein band corresponding to biotinylated Cch1 could not be detected.

currents directly in intact cells of *C. neoformans* and in yeast had failed. To express CMC in HEK293 cells, cDNA of *MID1* or *CCH1* was cloned into mammalian expression vectors, which were subsequently transfected into HEK293 cells. Detection of mRNA transcripts of Cch1 and Mid1 confirmed the expression of the channel in HEK293 cells that were previously transfected with *CCH1* and *MID1* (Fig. 1*A*). Transcripts of Cch1 and Mid1 were not detected in nontransfected HEK293 cells.

To assess the localization of CMC in HEK293 cells, confocal microscopy was performed. Cells expressing a Mid1-GFP fusion protein revealed a cell surface distribution of Mid1 that co-localized with Cch1 (Fig. 1*B*) (24). Western blot analysis of isolated plasma membranes from HEK293 cells expressing Cch1 or Mid1 revealed the presence of polypeptides corresponding to the predicted size of Cch1 and Mid1, suggesting that both proteins were indeed sufficiently expressed in HEK cells (Fig. 1*C*). Interestingly, under nonreducing conditions (the

absence of β-mercaptoethanol) two distinct protein bands were detected for Mid1 similar to that reported for Mid1 in yeast (40). The 100 kDa band represented the Mid1 monomer, and the 200 kDa band likely corresponded to a Mid1 complex (Fig. 1C) (40). This result suggested that Mid1 likely forms an oligomer through sulfide bonding similar to Mid1 in yeast (40).

To confirm further the expression of Cch1 and Mid1 on the surface of HEK293 cells, biotinylation was performed. Western blot analysis of biotin-labeled HEK293 cells expressing Cch1 or Mid1 revealed two distinct bands corresponding to the monomer and the complex forms of Mid1 (Fig. 1D) similar to that observed in Western blots of isolated plasma membranes from HEK cells expressing Mid1 (Fig. 1C). These distinct bands were not detected in biotinylated HEK cells that did not express Mid1 or Cch1 (nontransfected HEK cells). Unfortunately, Cch1 could not be detected in Western blots from biotinylated HEK cells expressing Cch1 (Fig. 1D). Because Cch1 is such a large and bulky protein based on its predicted structure (24 transmembrane domains), it is conceivable that steric hindrance may have masked surface lysine residues thus preventing sufficient biotin from attaching. Nevertheless, the biotinylation of Mid1 confirms its expression on the surface of HEK293 cells, and the co-localization of Mid1 with Cch1 strongly suggests that Cch1 is also expressed on the surface of HEK cells.

Cch1 Is Activated by the Depletion of Intracellular Ca^{2+} Stores—To assess whether Cch1-mediated Ca^{2+} currents were activated by passive Ca^{2+} store depletion, the Ca^{2+} chelator BAPTA-AM was added to the patch pipette. This uncharged molecule permeates cell membranes, and once inside the cell the lipophilic blocking groups are cleaved by nonspecific esterases resulting in a charged form that remains trapped within the cytosol (3). Consequently, ER Ca^{2+} stores are eventually depleted because the chelator captures released Ca^{2+}. Ramp protocols were used to measure the time-dependent development of Ca^{2+} currents through Cch1 in HEK293 cells expressing Cch1, Mid1, or both. Ca^{2+} store depletion resulted in the development of robust, time-dependent Cch1 channel currents with either Ca^{2+} or Ba^{2+} as the charge carrier. In this case, Ba^{2+} was used as a surrogate for Ca^{2+}, a common practice when measuring Ca^{2+} channels (25). Notably, Ba^{2+} currents developed slower than Ca^{2+} currents. This was probably due to secondary effects of Ba^{2+} blocking K^{+} conductances and affecting the electrical potential difference across the plasma membrane thus reducing the driving force for Ba^{2+} influx (Fig. 2, *A* and *B*) (25). Inward Ca^{2+} currents through Cch1 developed promptly in response to BAPTA-AM and spontaneously declined to resting levels (Fig. 2C).

The addition of the well characterized Ca^{2+} channel blockers such as nifedipine and verapamil did not block Cch1-mediated currents at physiological concentrations (data not shown). Some inhibition of Cch1 Ca^{2+} currents was observed in the presence of nifedipine but only at very high concentrations (10 mM), suggesting that CnCch1 probably lacks the classic binding site for dihydropyridines and phenylalkyamines. In contrast, the addition of 10 μM La^{3+} resulted in a 75% reduction in the time-dependent inward Ca^{2+} currents, indicating that La^{3+} blocked Cch1 channel activity (Fig. 2D). The La^{3+}-induced block of Ca^{2+} currents is a pharmacological hallmark of SOC
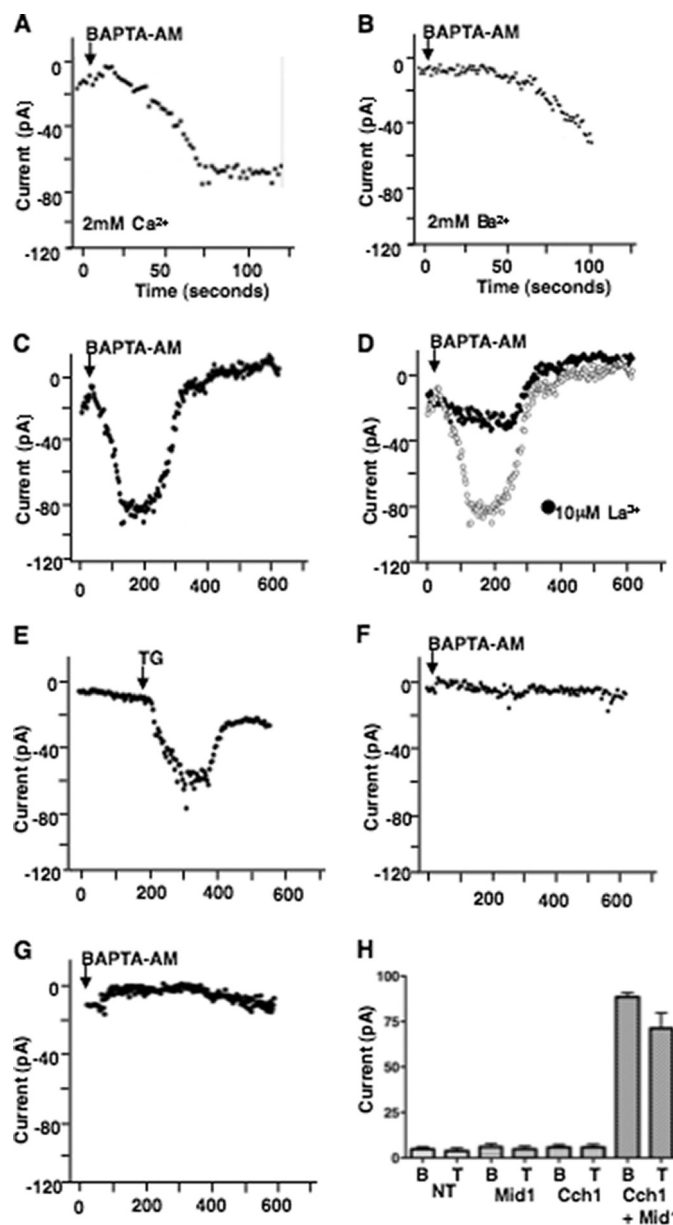
FIGURE 2. **Inward divalent currents through the Cch1 channel are activated by the depletion of Ca^{2+} stores.** *A–G*, representative traces of time course of whole cell Ca^{2+} currents through the Cch1 channel. *B*, trace of Ba^{2+} currents through Cch1. *C* and *E*, Ca^{2+} and Ba^{2+} currents measured upon the depletion of Ca^{2+} stores by the addition of 10 μM BAPTA-AM or with 100 μM thapsigargin (*TG*) in the patch pipette. *D*, 10 μM La^{3+} in the bath solution significantly reducing Ca^{2+} currents through Cch1. *F* and *G*, Ca^{2+} currents not detected in HEK293 cells expressing either Cch1 alone (*F*) or Mid1 alone (*G*). *H*, average of maximum Ca^{2+} current levels (-80 mV) measured in HEK293 cells alone (nontransfected, *NT*) or expressing Cch1, Mid1 or both ($n = 5$). Data are expressed as means $\pm$ S.D. (*error bars*).

channels (3, 4), further strengthening the functional similarity between CMC and SOC channels in mammalian cells.

Consistent with the stimulation of Ca^{2+} currents by chelation of Ca^{2+} from the ER, time-dependent inward Ca^{2+} currents through Cch1 also developed in response to thapsigargin (Fig. 2E). Thapsigargin, an inhibitor of the ER Ca^{2+}-ATPase pump, leads to the depletion of Ca^{2+} stores because as Ca^{2+} passively leaks from the ER, Ca^{2+} levels are no longer balanced by reuptake (26). Store depletion-mediated inward Ca^{2+} currents were not detected in HEK cells that expressed either Cch1

or Mid1 alone or an empty plasmid, indicating that the activation of these Ca^{2+} currents was completely dependent on the co-expression of Cch1 and Mid1 and that Cch1 activity required Mid1, consistent with previous genetic evidence (Fig. 2, *F–H*) (12, 14, 20, 21). Importantly, Mid1 did not conduct any Ca^{2+} currents on its own during passive Ca^{2+} store depletion. The mechanism underlying the action of Mid1 on Cch1 function remains unknown.

Cch1 Is Permeable to Both Ca^{2+} *and* Ba^{2+}—Macroscopic *I-V* curves demonstrated that depletion of Ca^{2+} stores by BAPTA-AM produced Cch1-mediated currents with either Ca^{2+} or Ba^{2+} as the charge carrier. Surprisingly, although Ca^{2+} and Ba^{2+} were both permeable, Ba^{2+} currents were steeply voltage-dependent. As membrane potentials became increasingly hyperpolarized, Ba^{2+} currents fell to a greater extent than Ca^{2+} currents, resulting in a more pronounced inward rectification (Fig. 3*A*). The Ca^{2+} or Ba^{2+} channel currents of Cch1 were not affected by the presence of the C-terminal GFP tag on the Cch1 protein as indicated by the *I-V* plot (Fig. 3*E*). In addition, currents were not detected in HEK cells expressing empty plasmids, strongly suggesting that the Ca^{2+} currents detected were mediated by Cch1 (Fig. 3*E*). The amplitude of Cch1-mediated currents at −40 mV with Ca^{2+} as the charge carrier was ~50% less than the amplitude measured at −80 mV (Fig. 3*B*). However, with Ba^{2+} the current amplitude at −40 mV was only ~10% of the current levels detected at −80 mV, indicating that Ba^{2+} permeation through Cch1 was voltage-dependent. We found that Ba^{2+} currents were negligible at membrane potentials depolarized beyond −60 mV, whereas Ca^{2+} currents were detected at these same potentials, reflecting the voltage independence of Ca^{2+} currents through Cch1 under physiological conditions.

The voltage dependence of Ba^{2+} currents through Cch1 was reflected in the ensemble average of single channel records consistent with the macroscopic *I-V* curves (Fig. 3*C*). Single channel events were not detected at −60 mV with Ba^{2+} as the charge carrier; however, channel activity increased dramatically at −80 mV, indicating the voltage dependence of single channel Ba^{2+} currents through Cch1 (Fig. 3*C*). Single channels exhibited long duration openings with a conductance of ~0.08 picosiemens in 10 mM Ba^{2+}, consistent with the small channel conductance reported for CRAC channels (27).

Cch1 Maintains High Ca^{2+} *Selectivity in the Presence of Monovalent Ions*—One of the distinguishing properties of SOC channels is their highly permeability to sodium ions and other monovalent ions in the absence of divalent cations (27). We sought to determine whether CMC shared this feature with SOC channels, and therefore we tested whether Cch1 was permeable to monovalent ions in the absence or presence of divalent cations. The reversal potential of the Ba^{2+} inward current (E_{Ba}) in 5 mM Ba^{2+} was +42 ± 2 mV and +58 ± 2 mV for the Ca^{2+} inward current (E_{Ca}) in 5 mM Ca^{2+} (Fig. 3*A*). These values were far less positive than the predicted E_{Ba} and E_{Ca} values for experimental conditions where extracellular [Ca^{2+}] and [Ba^{2+}] were about 10^5 times higher than the [Ca^{2+}] and [Ba^{2+}] inside the patch pipette. These results indicated that Cs$^+$ carried some outward current through Cch1 and in doing so made a significant contribution to the reversal potential of Cch1 by

shifting the E_{Ba} and E_{Ca} to less positive values. However, Cch1 was more selective for Ca^{2+} than Ba^{2+} because E_{rev} was more positive and closer to the equilibrium potential for Ca^{2+}. Interestingly, Na$^+$ conductance through Cch1 in the absence of divalent cations was negligible, and the addition of Ca^{2+} in the presence of Na$^+$ resulted in large inward currents with a shift in E_{rev} to positive potentials approaching E_{Ca} (Fig. 3*D*). These results indicated that unlike some SOC channels in higher eukaryotes that are highly permeable to Na$^+$ in the absence of divalent cations, Cch1 is weakly permeable to Na$^+$ and maintains a strong Ca^{2+} selectivity even in the presence of high [Na$^+$] (4, 27).

Cryptococcal Cells Require Cch1 Activity to Survive ER Stress—To test the physiological role of the channel, strains of *C. neoformans* lacking a functional CMC were constructed and tested for survival with ER-stressing agents. To single out the requirement for CMC in low [Ca$^+$], ER-stressing agents were added to YPD medium (free [Ca^{2+}] ~0.140 mM) where the free [Ca^{2+}] was reduced to ~500 nM with a cell-impermeable form of a Ca^{2+} chelator (BAPTA) (28, 29). Lowering [Ca^{2+}] further rendered the CMC mutants inviable, but at ~500 nM, low affinity Ca^{2+} channels and/or transporters allow for Ca^{2+} influx that supports viable CMC mutants (7, 20). In the presence of the ER-stressing agent tunicamycin, a wild type strain of *C. neoformans* showed no significant growth defect with the exception of the *mid1Δ* mutant (Fig. 4, *A* and *E*); however, the growth of *C. neoformans* strains lacking a functional CMC was severely compromised. The *cch1Δ* and *mid1Δ* single null mutants and the *cch1Δmid1Δ* double mutants were not viable when exposed to tunicamycin in low extracellular [Ca^{2+}] (Fig. 4, *B* and *F*). A similar phenotype was observed in the presence of fluconazole or ketoconazole, drugs belonging to the azole class of antifungals (Fig. 4, *C*, *D*, *G*, and *H*) (30, 31). These results indicated that cryptococcal cells required CMC to survive ER stress conditions and supported the notion that the Cch1 channel plays an essential role in reestablishing Ca^{2+} homeostasis.

DISCUSSION

The results presented here demonstrate that the Cch1-Mid1 proteins constituted a functional Ca^{2+} channel in HEK293 cells that exhibited some features inherent to the non-voltage-gated SOC channels. This first mechanistic study of Cch1 indicates that it is a Ca^{2+}-selective SOC channel that is gated by the depletion of intracellular Ca^{2+} based on the following observations: (i) inward Ca^{2+} currents were activated upon the passive depletion of Ca^{2+} with BAPTA-AM and thapsigargin at negative membrane potentials; (ii) Cch1 was permeable to Ba^{2+} ions; and (iii) Ca^{2+} currents were blocked by La^{3+}.

It is known that in eukaryotes the ER constitutes a finite reservoir of Ca^{2+} primarily mobilized for signaling that must be replenished to sustain the duration of signaling and ultimately restore Ca^{2+} homeostasis in the ER and the cytosol (1–3, 32). In *C. neoformans* mediators of the Ca^{2+} signaling pathway, such as calcineurin, calmodulin, and the sarco (endo)plasmic reticulum Ca^{2+}-ATPase are central to maintaining intracellular Ca^{2+} homeostasis while withstanding the multitude of stresses imposed by the host (33). ER stress can be detrimental to fungal cells if ER function is not restored because in addition to its
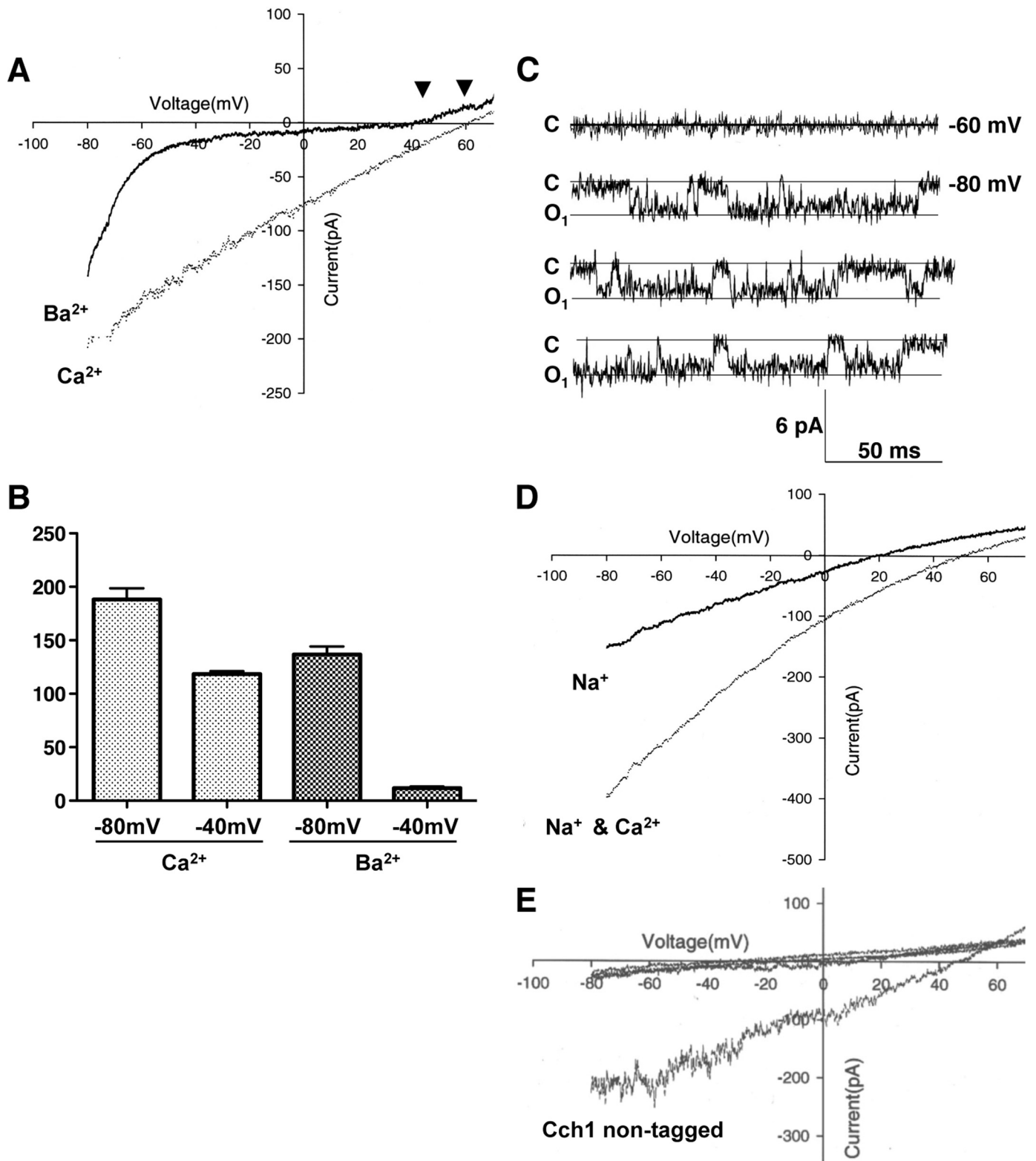
FIGURE 3. **Divalent and monovalent inward currents through the Cch1 channel in HEK293 cells.** *A*, whole cell currents revealed that Cch1 is permeable to both Ca^{2+} (5 mM) and Ba^{2+} (5 mM). *Arrows* indicate E_{rev} (reversal potential) for E_{Ca} and E_{Ba}. Inward current is carried by Ca^{2+} or Ba^{2+}, and outward current above +40 mV is carried by Cs^{+}. *B*, Ba^{2+} currents are voltage-dependent, whereas Ca^{2+} currents are voltage-independent. Current levels for Ca^{2+} and Ba^{2+} measured at −80 mV and −40 mV were plotted (*n = 5*). Data are expressed as means ± S.D. (*error bars*). *C*, representative single channel record of single channel Ba^{2+} currents through Cch1. Single channels exhibited long duration openings and a small channel conductance (~0.08 picosiemens). *D*, weak Na^{+} current through the Cch1 channel in the absence of divalent cations. Cch1 maintains a high Ca^{2+} selectivity in the presence of Ca^{2+} and high [Na^{+}]. *E*, Ca^{2+} or Ba^{2+} currents were not detected in HEK cells that had been transfected with empty plasmids as shown in the current-voltage (*I-V*) plot. In addition, the presence of a C-terminal GFP tag on Cch1 did not alter the channel kinetics of Cch1 as shown from the *I-V* plot measured from HEK cells expressing Cch1 without a GFP tag. *E*, Ca^{2+} or Ba^{2+} channel currents of Cch1 were not affected by the presence of the C-terminal GFP tag on the Cch1 protein as indicated by the *I-V* plot. Currents were not detected in HEK cells expressing empty plasmids (2) or in nontransfected HEK cells (indicated by flat *I-V* plots).
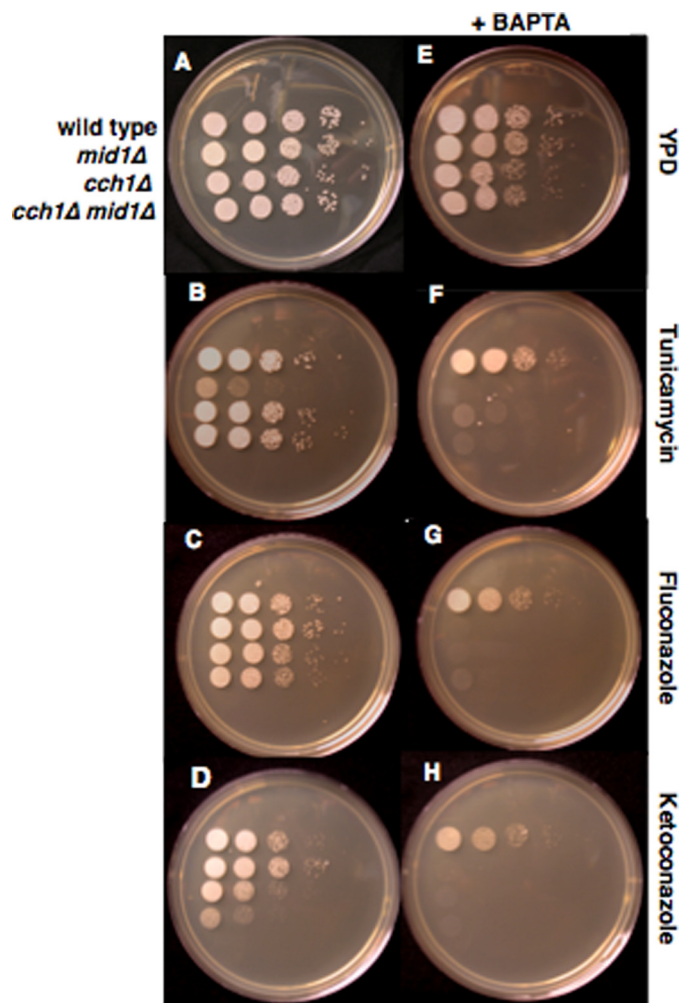
FIGURE 4. **Cch1-Mid1 channel is essential for the survival of cryptococcal cells during ER stress.** Sensitivity spot assays were used to evaluate the requirement for Cch1 and Mid1 in *C. neoformans* during drug-induced ER stress conditions. *A–D*, serially diluted cells (10^6, 10^5, 10^4, 10^3, 10^2) from wild type, *mid1Δ*, *cch1Δ*, and *cch1Δmid1Δ*-null mutant strains of *C. neoformans* were added to YPD agar plates with ER-stressing agents, tunicamycin (75 ng/ml), fluconazole (8 μg/ml), and ketoconazole (180 ng/ml). *E–H*, ER-stressing agents were added to YPD plates supplemented with BAPTA (cell-impermeant), and spot assays were performed as explained above.

crucial role in the posttranslational processing of proteins, the ER is also a key player in Ca^{2+} signaling (32). Here, we show that Cch1 activity plays an essential role in the survival of cryptococcal cells in response to ER stress by coupling the depleted state of ER Ca^{2+} stores to the influx of Ca^{2+} across the plasma membrane. The presence of a specific Ca^{2+} chelator and an inhibitor of the Ca^{2+}-ATPase, both capable of depleting intracellular ER Ca^{2+} stores, led to the development of Ca^{2+} inward currents at negative membrane potentials, indicating that Cch1 functions primarily to replenish these stores and reestablish Ca^{2+} homeostasis. This is supported by studies in yeast that have suggested that the Cch1-Mid1 channel likely promotes the influx of Ca^{2+} during depletion of secretory Ca^{2+} and that this activity was necessary for yeast survival during ER-stressing conditions (17, 18, 20). The electrophysiological evidence provided here strongly supports a Ca^{2+} depletion gating mechanism for Cch1 and further substantiates a role for Cch1 in the process of SOC entry in lower eukaryotes (20).

Similar to other Ca^{2+} channels in higher eukaryotes, Cch1 was also highly permeable to barium ions. Unexpectedly, Ba^{2+} movement through Cch1 was voltage-dependent; however, Ca^{2+} influx was not. This suggested that very hyperpolarized potentials were probably needed to displace Ba^{2+} bound to the Cch1 pore with an incoming Ba^{2+} ion likely due to weak electrostatic repulsion between Ba^{2+} ions, thus resulting in the voltage dependence of Ba^{2+} influx (25). Interestingly, CRAC channels, a subtype of the voltage-independent SOC channels in mammalian cells, also exhibit a similar voltage-dependent influx of Ba^{2+} at negative membrane potentials (34). Our results indicate that Cch1 is not voltage-gated, and this is further supported by our previous findings demonstrating that the protein sequence of Cch1 in *C. neoformans* lacks the highly conserved voltage sensor motif, the hallmark of all voltage-gated channels in eukaryotic cells (7, 35–37). Moreover, the recently characterized NALCN neuronal Na^+ channel, which like CnCch1 has fewer positively charged amino acids (lysine and arginine) within its voltage-sensing S4 segment and thus lacks a *bona fide* voltage sensor, was found to be voltage-independent (38).

The activation of Cch1-mediated Ca^{2+} currents required the presence of Mid1, indicating that Cch1 cannot promote Ca^{2+} influx independently of Mid1. This is consistent with previous genetic data that demonstrated identical phenotypic defects of strains lacking either Mid1 or Cch1 including nonviability in low [Ca^{2+}] medium (7, 11, 15, 20). Despite the noted requirement for Mid1, its role in the functional regulation of the Cch1 channel remains unknown. Our results rule out the possibility that Mid1 is involved in the trafficking of Cch1 to the plasma membrane because Cch1 was clearly expressed in the plasma membrane of HEK293 cells independently of Mid1. In addition, recent evidence has demonstrated that the localization of Cch1 to the plasma membrane in cryptococcal cells is dependent on an elongation factor (EF3), further suggesting that Mid1 is excluded from this process (14). Under Ca^{2+}-depleted conditions, Mid1 did not promote the influx of divalent cations when expressed on its own, indicating that Mid1 does not have any independent channel activity under these particular conditions (39). It is conceivable that Mid1 may be coupling the depleted state of intracellular Ca^{2+} to the activity of Cch1. This is a particularly appealing notion based on the pivotal role of STIM1 in the activation of Orai1, a non-voltage-gated, store-operated Ca^{2+}-selective channel in mammalian cells (5). However, although Mid1 appears to have a predicted ER retention signal it does not contain any predicted Ca^{2+} sensor domains thus if Mid1 did function in this role, other proteins would also likely be involved.

In summary, the SOC gating mechanism of Cch1 indicates that the Cch1 channel functions primarily to replenish depleted Ca^{2+} levels and reestablish Ca^{2+} homeostasis. This enables *C. neoformans* to overcome ER stress-mediated events that are likely rampant during infection and colonization of the host.

REFERENCES

1. Putney, J. W., Jr. (1986) *Cell Calcium* **7,** 1–12
2. Putney, J. W., Jr. (1990) *Cell Calcium* **11,** 611–624
3. Hogan, P. G., and Rao, A. (2007) *TRENDS Biochem. Sci.* **32,** 235–245
4. Parekh, A. B., and Putney, J. W., Jr. (2005) *Physiol. Rev.* **85,** 757–810
5. Zhang, S. L., Yu, Y., Roos, J., Kozak, J. A., Deerinck, T. J., Ellisman, T. H., Stauderman, K. A., and Cahalan, M. D. (2005) *Nature* **437,** 902–905
6. Feske, S., Gwack, Y., Prakriya, M., Srikanth, S., Puppel, S. H., Tanasa, B., Hogan, P. G., Lewis, R. S., Daly, M., and Rao, A. (2006) *Nature* **441,** 179–185
7. Liu, M., Du, P., Heinrich, G., Cox, G. M., and Gelli, A. (2006) *Eukaryot. Cell* **5,** 1788–1796
8. Paidhungat, M., and Garrett, S. (1997) *Mol. Cell. Biol.* **17,** 6339–6347
9. Hallen, H. E., and Trail, F. (2008) *Eukaryot. Cell* **7,** 415–424
10. Zelter, A., Bencina, M., Bowman, B. J., Yarden, O., and Read, N. D. (2004) *Fungal Genet. Biol.* **41,** 827–841
11. Fischer, M., Schnell, N., Chattaway, J., Davies, P., Dixon, G., and Sanders, P. (1997) *FEBS Lett.* **419,** 259–262
12. Mitchell, T. G., and Perfect, J. R. (1995) *Clin. Microbiol. Rev.* **8,** 515–548
13. Casadevall, A., and Perfect, J. R. (1998) *Cryptococcus neoformans.* American Society for Microbiology, Washington, D. C.
14. Liu, M., and Gelli, A. (2008) *Eukaryot. Cell* **7,** 1118–1126
15. Iida, H., Nakamura, N., Ono, T., Okumura, M. S., and Anraku, Y. (1994) *Mol. Cell. Biol.* **14,** 8259–8271
16. Kaur, R., Castaño, I., and Cormack, B. P. (2004) *Antimicrob. Agents Chemother.* **48,** 1600–1613
17. Bonilla, M., and Cunningham, K. W. (2003) *Mol. Biol. Cell.* **14,** 4296–4305
18. Bonilla, M., Nastase, K. K., and Cunningham, K. W. (2002) *EMBO* **21,** 2343–2353
19. Edlind, T., Smith, L., Henry, K., Katiyar, S., and Nickels, J. (2002) *Mol. Microbiol.* **46,** 257–268
20. Locke, E. G., Bonilla, M., Liang, L., Takita, Y., and Cunningham, K. W. (2000) *Mol. Cell. Biol.* **20,** 6686–6694
21. Hamill, O. P., Marty, A., Neher, E., Sakmann, B., and Sigworth, F. J. (1981) *Pflugers Arch. Eur. J. Physiol.* **391,** 85–100
22. Vu, K., Bautos, J., Hong, M. P., and Gelli, A. (2009) *Anal. Biochem.* **393,** 234–241
23. Davidson, R. C., Cruz, M. C., Sia, R. A. L., Allen, B., Alspaugh, J. A., and Heitman, J. (1999) *Fungal Genet. Biol.* **29,** 38–48
24. Vergara, C., Latorre, R., Marrion, N. V., and Adelman, J. P. (1998) *Curr. Opin. Neurobiol.* **8,** 321–329
25. Hille, B. (1992) *Ionic Channels of Excitable Membranes*, 2nd Ed, Sinauer Associates Inc., Sunderland, MA
26. Rogers, T. B., Inesi, G., Wade, R., and Lederer, W. J. (1995) *Biosci. Rep.* **15,** 341–349
27. Kerschbaum, H. H., and Cahalan, M. D. (1999) *Science* **283,** 836–839
28. Tsien, R. Y. (1980) *Biochemistry* **19,** 2396–2404
29. Marks, P. W., and Maxfield, F. R. (1991) *Anal. Biochem.* **193,** 61–71
30. Odds, F. C., Brown, A. J. P., and Gow, N. A. R. (2003) *Trends Microbiol.* **11,** 272–279
31. Kauffman, C. A. (2006) *Curr. Opin. Microbiol.* **9,** 483–488
32. Brostrom, M. A., and Brostrom, C. O. (2003) *Cell Calcium* **34,** 345–363
33. Fan, W., Idnurm, A., Breger, J., Mylonakis, E., and Heitman, J. (2007) *Infect. Immun.* **75,** 3394–3405
34. Bakowski, D., and Parekh, A. B. (2007) *Cell Calcium* **42,** 333–339
35. Catterall, W. A. (2000) *Annu. Rev. Cell Dev. Biol.* **16,** 521–555
36. Durrell, S. R., Shrivastava, I. H., and Guy, H. R. (2004) *Biophys. J.* **87,** 2116–2130
37. Long, S. B., Campbell, E. B., and MacKinnon, R. (2005) *Science* **309,** 903–908
38. Lu, B., Su, Y., Das, S., Liu, J., Xia, J., and Ren, D. (2007) *Cell* **129,** 371–383
39. Kanzaki, M., Nagasawa, M., Kojima, I., Sato, C., Naruse, K., Sokabe, M., and Ida, H. (1999) *Science* **285,** 882–886
40. Yoshimura, H., Tada, T., and Ida, H. (2004) *Exp. Cell Res.* **293,** 185–195